Taira A., Hill I., Firth, J., et al., 1991
Proceedings of the Ocean Drilling Program, Initial Reports, Vol. 131

1. GEOLOGICAL BACKGROUND AND OBJECTIVES[1]

Shipboard Scientific Party[2]

INTRODUCTION

The accretion of sediments in oceanic trenches is an initial step in the process of mountain building and continental crustal growth. The product of sediment accretion at a trench, the accretionary prism, has therefore been an important constituent of orogenic belts throughout earth history. In accretionary prisms, sediment deformation, physical property changes, diagenetic alteration, and fluid migration occur in a complex manner, very different from ordinary sedimentary basins. Understanding of the interplay of these processes is a major objective of modern land geology as well as an attractive ocean-drilling target (see Moore and Lundberg, 1986 for review).

With respect to the origin and evolution of accretionary prisms, quantity and type of sediment input seem to play an important role (Moore and Lundberg, 1986). Among the well-documented examples of modern accretionary prisms, two basic types exist: coarse clastic (sand and silt) dominated prisms and clay-dominated prisms. Most modern prisms such as Nankai, Cascadia, Makran, Aleutian, Manila, Sunda, Middle America off southern Mexico, and southern Barbados fall into the first category, being dominated by turbidite and hemipelagic sediment input. The second type of prism, dominated by pelagic/hemipelagic sediments with little turbidite input, is relatively rare. A well-documented example is that of northern Barbados. It is generally inferred that there are basic differences in hydrogeology and physical property evolution between the two contrasting prism types. In a coarse clastic prism, intergranular permeability may play an important role whereas in a clay prism, fracture permeability may be the dominant effect (Moore, 1989). Porosity loss in mudstone seems faster in clastic prisms than in clay prisms, thus providing a contrasting history of consolidation characteristics and fluid expulsion processes (Marlow et al., 1984; Bray and Karig, 1985; Karig, 1986).

In the history of deep-sea drilling, three accretionary prisms have been investigated: northern Barbados, Middle America and Nankai. The northern Barbados accretionary prism was drilled during Leg 78A (Biju-Duval, Moore et al., 1984) and 110 (Moore et al., 1988; Mascle and Moore et al., 1988), with successful penetration of the décollement (detachment zone). The results of these previous Barbados legs provide important information on the structure and hydrogeology of a clay prism. However, the nature of the more abundant clastic prism type has not yet been investigated in detail. Deep-sea drilling legs at Middle America (Leg 66, Watkins, Moore et al., 1982) and Nankai (Leg 31, Karig, Ingle, Jr., et al., 1975; Leg 87, Kagami, Karig, Coulbourn et al., 1986) focused on the structural evolution of the clastic prisms. The results of these legs were, however, insufficient to demonstrate the interaction of structural styles, fabrics, diagenesis and fluid behavior. Moreover, *in-situ* measurements of various physical and mechanical properties of an accretionary prism have not been achieved. These parameters have a fundamental importance in understanding the physical processes of an accretionary prism (e.g., Davis et al., 1983; Shi and Wang, 1988).

The Nankai Trough is one of the best places to achieve the study of a clastic prism because (1) substantial site survey data exist, including excellent images of the three-dimensional geologic structures by seismic profiling, Sea Beam mapping, and IZANAGI long-range side-scan sonar survey (Aoki et al., 1982, 1986; Nasu, et. al., 1982; Kaiko I Research Group, 1986; Moore et al., 1990; Le Pichon, Iiyama, et al., 1987a, 1987b; Ashi et al, 1989); (2) the décollement is relatively shallow (1000 m below seafloor at the toe) and can be penetrated with present drilling technology; (3) the trench sediments are sandy turbidites that represent a modern type example of most ancient accretionary prisms (e.g., Shimanto Belt, Taira, Katto, et al., 1988; Southern Upland, Leggett et al., 1982; Franciscan Complex, Aalto, 1982; Kodiak Island, Byrne, 1984, Fisher and Byrne, 1988); (4) evidence of fluid migration and its surface manifestation has been documented by heat-flow measurements, bottom-simulating reflector (BSR) distribution and seep ecological community (Yamano et al., 1982; Le Pichon, Iiyama et al, 1987a); (5) high heat flow provides an opportunity to study large gradients in diagenesis; and (6) an almost direct ancient analog is exposed on land (Shimanto accretionary prism), providing an opportunity for comparative study.

GEOLOGIC AND TECTONIC BACKGROUND

The Nankai Trough is a topographic manifestation of the subduction boundary between the Shikoku Basin and the Southwest Japan Arc (Fig. 1). The Shikoku Basin is a part of the Philippine Sea Plate, which is moving to the northwest. This relative motion has a magnitude of 4 cm/yr as estimated from seismic slip vector (Seno, 1977) or 2 cm/year or less as estimated from trench wedge age (Karig and Angevine, 1986). To the east, the trough converges with a major arc-arc collision boundary between Honshu Island and the Izu-Bonin Arc (Fig. 2). The Wadati-Benioff zone extends only to a depth of 50 km, but further slab penetration has been inferred from observations of a high *P*-wave velocity channel (Shiono, 1988).

Active sediment accretion is presently taking place at the Nankai Trough and this has also been an important mechanism for crustal growth of the Japanese island arcs and the eastern margin of Asia in the geologic past (Taira and Tashiro, 1987). The basement rocks of the Southwest Japan Arc are mostly composed of ancient accretionary prisms of Paleozoic to Tertiary age (Taira et al., 1989) intruded and covered by Mesozoic to Holocene igneous rocks (Fig. 3).

Along the Pacific coastal zone of the Southwest Japan Arc and Ryukyu Arc is a belt of Cretaceous to Tertiary age accretionary prism called the Shimanto Belt that is characterized by imbricated thrust piles of trench turbidites and

[1] Taira, A., Hill, I., Firth, J., et al., 1991. *Proc. ODP, Init. Repts.,* 131: College Station, TX (Ocean Drilling Program).

[2] Shipboard Scientific Party is as given in the list of participants preceding the contents.

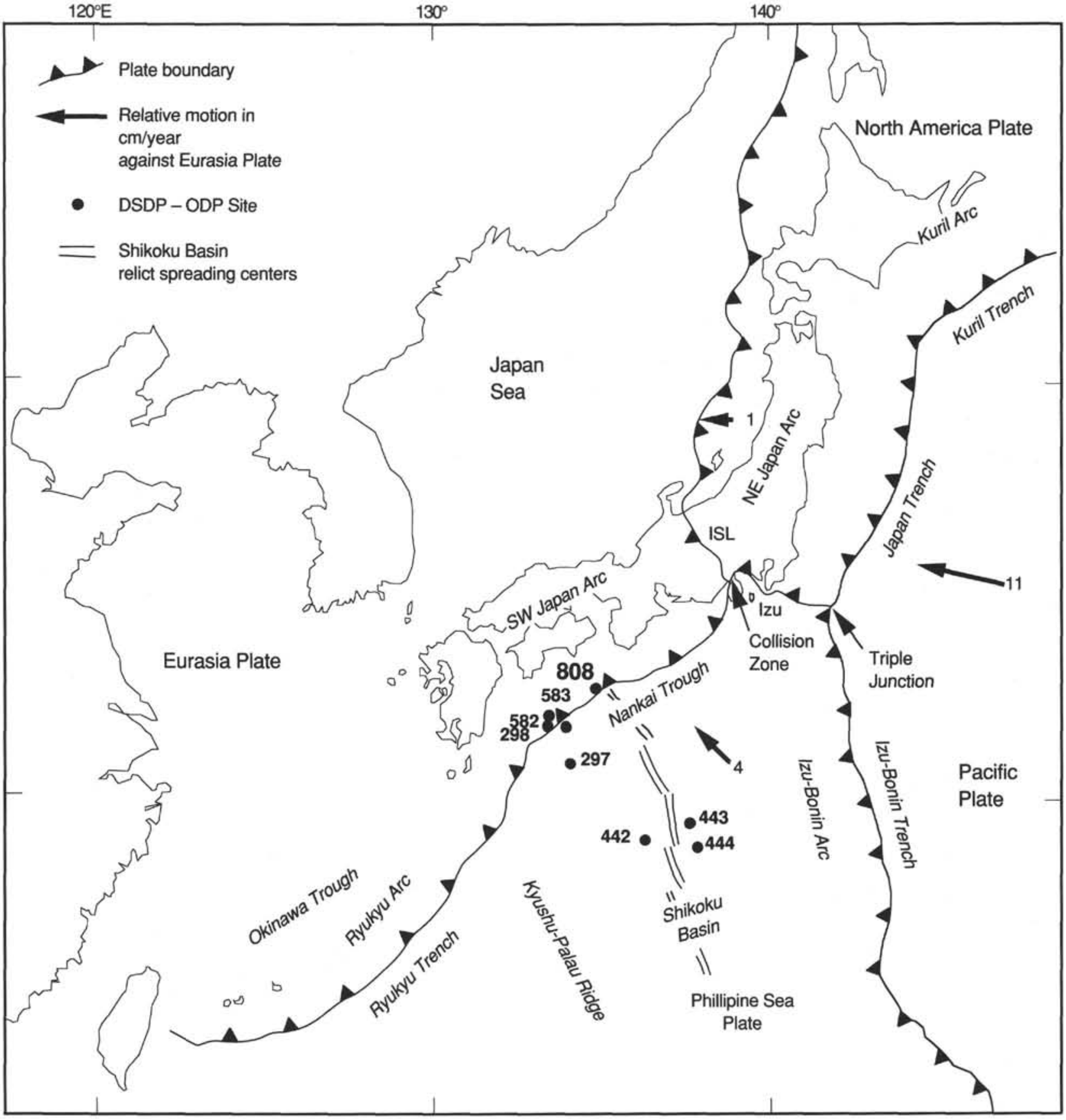

Figure 1. Tectonic setting of the Japanese arc-trench systems, showing the locations of major arc-trench systems, plate boundaries, and names of plates. ISL stands for Itoigawa-Shizuoka Tectonic Line. Location of DSDP and ODP sites and the spreading center of the Shikoku Basin are also shown.

mélanges comprising ocean floor basalts, seamount basalts and reef limestones, pelagic radiolarian chert and shale, and hemipelagic shale (Taira, Katto, et al., 1988). The youngest part of the exposed Shimanto Belt is lower Miocene, and is a product of plate subduction along the eastern margin of the Asian continent before the opening of the Japan Sea. The Shimanto Belt is interpreted as a direct ancient analog of the Nankai accretionary prism when one considers the age of subducted oceanic lithosphere, trench turbidite thickness, style of structure, and burial depth. To the south, the Shimanto Belt grades into a younger accretionary prism that was formed mostly after the opening of the Sea of Japan (see Fig. 3). The most recent part can be called the Nankai accretionary prism, which composes the trench landward slope and was created by the subduction of the Shikoku Basin.

The Shikoku Basin was formed as a backarc basin behind the Izu-Bonin Arc by mostly east–west-directed spreading, accompanied by a late-phase northeast–southwest spreading episode, during the late Oligocene to middle Miocene (25 to 15 Ma) (Kobayashi and Nakada, 1978; Shih, 1980; Chamot-Rooke et al, 1987). The fossil spreading center lies in the central part of the Shikoku Basin and is being subducted at the central part of the Nankai Trough.

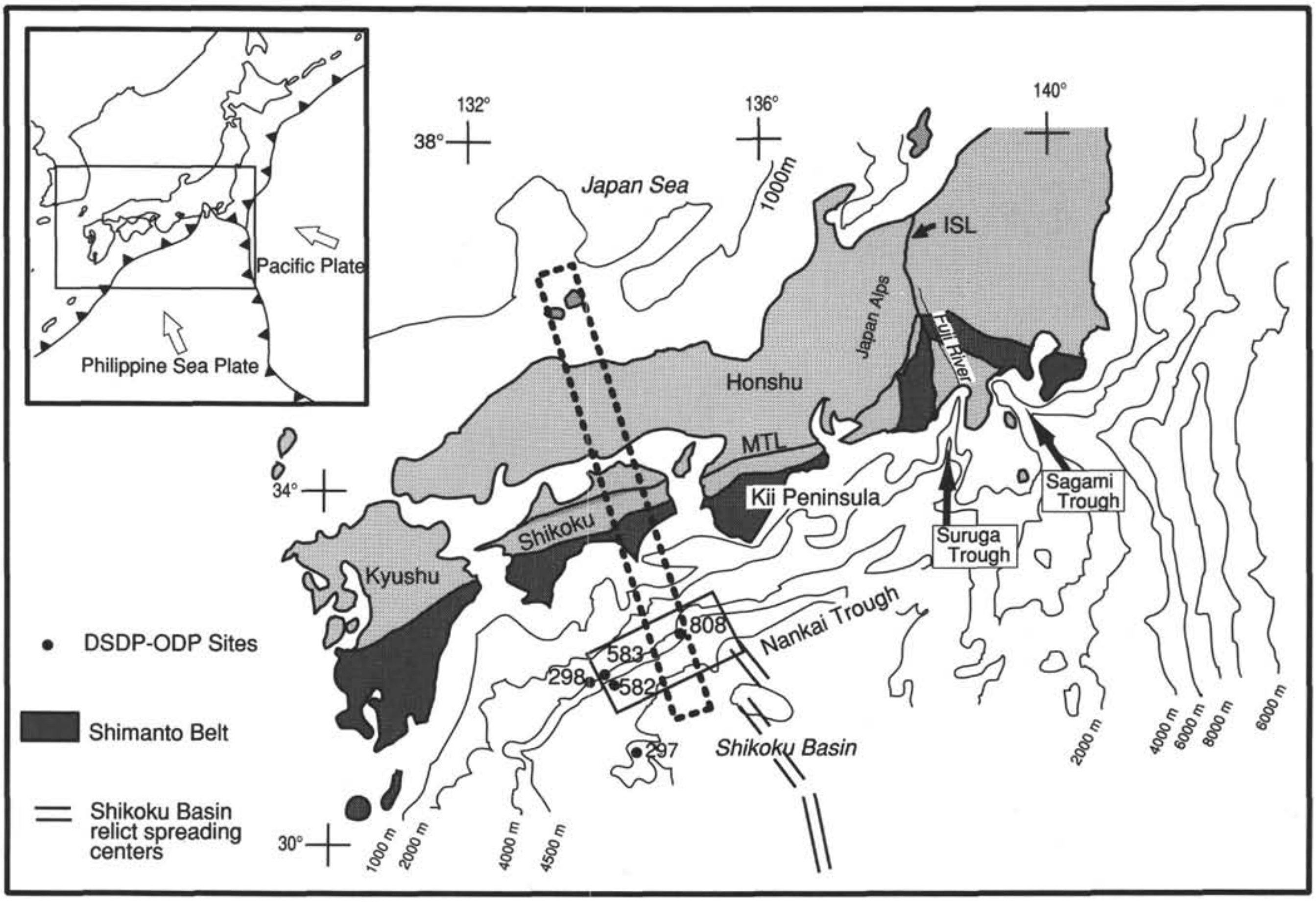

Figure 2. Tectonic and morphologic setting of Japanese Islands and Nankai Trough. The Nankai Trough is a subduction zone where the Shikoku Basin is underthrust beneath southwest Japan. The Nankai Trough converges to the Suruga Trough and the Izu collision zone. The Shimanto Belt is a Cretaceous-Tertiary accretionary complex. It is bounded by a major thrust and is separated from a Jurassic accretionary complex to the north. The Median Tectonic Line (MTL) has been interpreted to show a history of activity since the Cretaceous. It is presently a right-lateral strike-slip fault. DSDP and ODP sites are shown as solid circles. Location of the geotraverse (Fig. 3) is shown as a broken line. A rectangle at the Nankai Trough indicates the location of the Sea Beam map shown in Figure 4.

The Nankai Trough is shallow, with the maximum water depth being 4900 m. The shallowness of the trough can be attributed to two factors: the young age (Oligocene-Miocene) of the Shikoku Basin and the thick sediment pile in the trough. Beneath the sediment cover, the oceanic basement depth reaches 6000 m.

The sediments that are being brought to the deformation zone are composed of two sequences: an upper turbidite layer and a lower hemipelagic layer (Kagami, Karig, and Coulbourn, et al., 1986). The turbidites have been transported laterally along the axis of the trough from the mountain ranges of the arc-arc collision zone (Taira and Niitsuma, 1986). The sedimentation rate in the trough is enormous, exceeding 1 km/m.y. The thickness of the trench turbidite layer varies from place to place, chiefly owing to the configuration of the ocean basin (Le Pichon, Iiyama, et al., 1987a). At the central Nankai Trough, ridge-transform basement topography produced local ponding of turbidites in the trough by acting as dams for axial turbidity currents. Owing to this effect upon the axial turbidity current originating from the east, and the general shallowness over the fossil spreading axis, the trench turbidite layer is thinner at the drill sites.

The scenario that produced the Nankai accretionary prism can be summarized as follows. During the final stage of opening of the Shikoku Basin, the Sea of Japan also formed, and the Japanese island arc was created. The subduction of the Shikoku Basin and collision of the Izu-Bonin Arc followed the backarc opening events. The arc-arc collision produced crustal imbrication and uplift of the central Japan mountain range (Japan Alps), which served as a main sediment source for the trench. The trench turbidites together with the hemipelagic sequences are continuously being added to the deformation zone, forming a typical clastic-dominated accretionary prism.

PREVIOUS DRILLING

DSDP legs scientists in the Nankai Trough region drilled three sites in the trough and on the slope, all of which are west of the present sites. Site 298 penetrated 611 m at the toe of the prism, in a water depth of 4659 m. The total length of spot-cored section was 145.5 m with 46% recovery of the cored interval (Karig, Ingle, Jr., et al., 1975). The drilled section was mostly composed of turbidites with an overall coarsening upward trend. The hemipelagic sequence of the Shikoku Basin ocean floor was drilled at DSDP Site 297. The lithology encountered at this site showed that within these hemipelagic sediments there is a zone of relatively coarse-grained sediments (mud intercalated with silt and sand) at 350–550 meters below sea floor (mbsf), which is considered to be mostly of early Pliocene age (Karig, Ingle, Jr., et al., 1975).

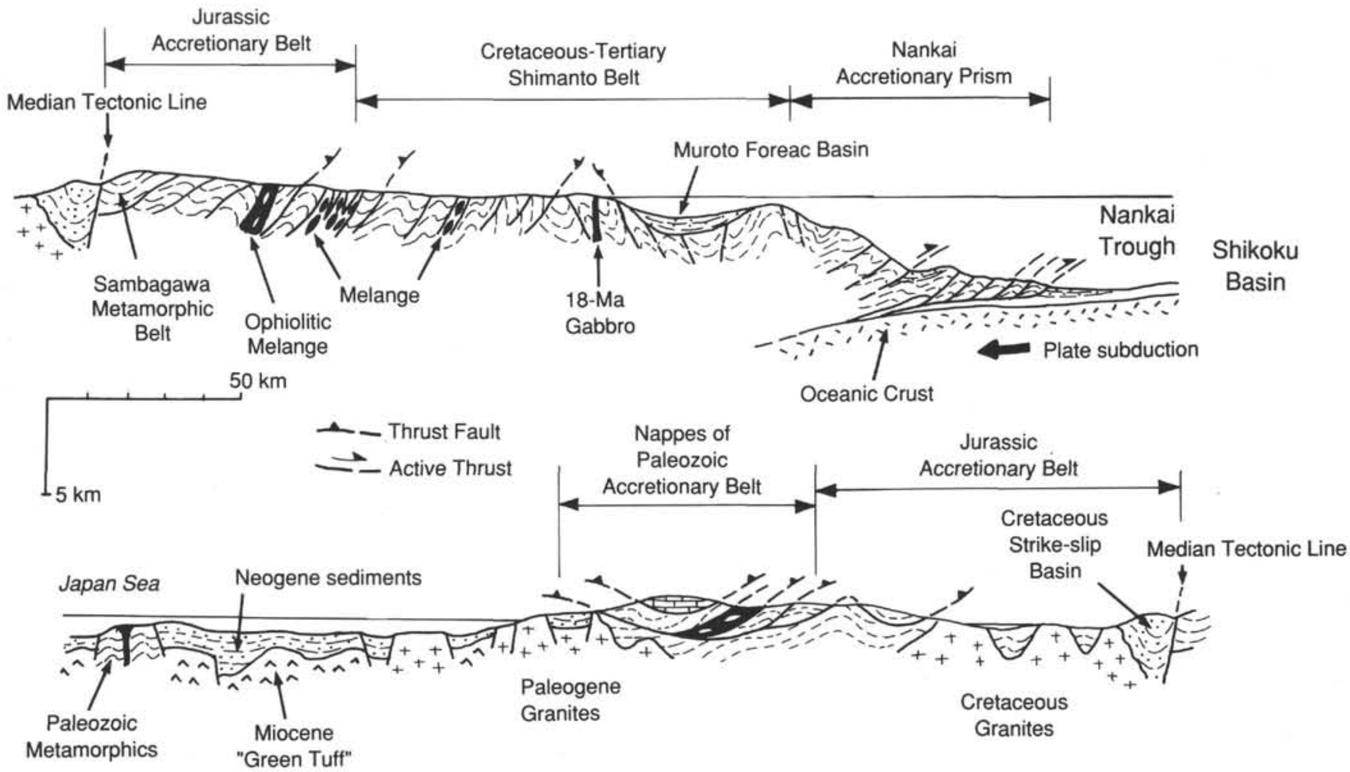

Figure 3. Schematic cross section of the Southwest Japan Arc. Honshu and Shikoku Islands are composed of thrust piles of Paleozoic to Tertiary accretionary complex. The Median Tectonic Line separates the Southwest Japan Arc basement rocks as the Inner Belt (Japan Sea side) and the Outer Belt (Pacific side). The Cretaceous-Paleogene granitic intrusives are only present in the Inner Belt (after Taira et al., 1989).

The lower part of the hemipelagic unit was recovered during DSDP Leg 58 at Site 443 in the more southern part of the Shikoku Basin, where the Miocene sequence was composed of mud, tuff, and basaltic sills (Curtis et al., 1980).

During Leg 87, Site 582 was drilled into the undeformed trench fill, with a maximum penetration of 750 m. The turbidite sequence at this site is 550 m thick and is underlain by lower Pleistocene to Pliocene hemipelagic sediment. Core recovery was 41%. Individual turbidites are composed of a graded unit of mostly medium to very fine-grained sand at the base, which grades to silt at the top. The mean thickness of each turbidite is 30 cm, intercalated with hemipelagic mud with a mean thickness of 5 cm (Taira and Niitsuma, 1986). Some individual turbidite sand layers reach 2 m in thickness. The hemipelagic sediments underneath the turbidites are composed mostly of bioturbated mud intercalated with volcanic ash.

Site 583 was drilled at the toe of the prism and using eight holes achieved maximum penetration of 450 m and overall core recovery of 77%. The upper parts of three holes at Site 583 were hydraulically piston cored to 60 mbsf. These sediments were typically fine-grained hemipelagic mud, divided into beds about 10 cm thick, with individual beds commonly separated by layers of sand and vitric ash. The oldest sediments recovered at Site 583 are Quaternary. Hole 583F was also logged continuously for 200 m. The temperature gradient in the upper 200 m of sediment at Site 583 was 5°C/100 m (Kinoshita and Yamano, 1986).

Scientists on Leg 87 attempted to compare undeformed vs. deformed sediments, but failed due to insufficient penetration in the deformation zone. Lack of success was primarily caused by mechanical failure and weather deterioration.

STRUCTURE OF THE NANKAI ACCRETIONARY PRISM

The structure of the Nankai accretionary prism has been studied extensively by Sea Beam mapping (Figs. 4 and 5), IZANAGI sidescan imaging (Fig. 6), and seismic profiling. The selection of the drill site of Leg 131 was based on multichannel seismic lines obtained by the *Fred Moore* during United States-Japan two-ship seismic experiments (Backpocket Fig. 2, Chapter 2, this volume). As a detailed discussion of the structure of the Nankai accretionary prism in a regional context will be presented elsewhere, the structure in the vicinity of the Leg 131 drill site is described based on the discussion presented by Moore et al. (1990).

The structure found in the western Nankai accretionary prism toe, west of approximately 137°E, is uniform on a gross scale and is characterized by two structural zones; the proto-thrust zone and the imbricate thrust zone. The proto-thrust zone designates an initial feature of deformation represented by seaward tilting of the trench wedge, development of small displacement reverse faults and thickening of the sedimentary section. This general thickening of the sedimentary section, especially within the hemipelagic section, has been attributed to ductile flow within the sedimentary section (Karig and Lundberg, 1990). The proto-thrust zone is followed by development of a major thrust, usually with vertical displacement of 50 to 200 m, which is manifested at the seafloor by a linear topographic ridge marking an initiation of the imbricate thrust zone. In some of the seismic profiles this fault zone is clearly imaged by a reflection, and even the second and third thrusts further landward can be traced by their seismic image. In many seismic sections, thrust reflections die out landward and

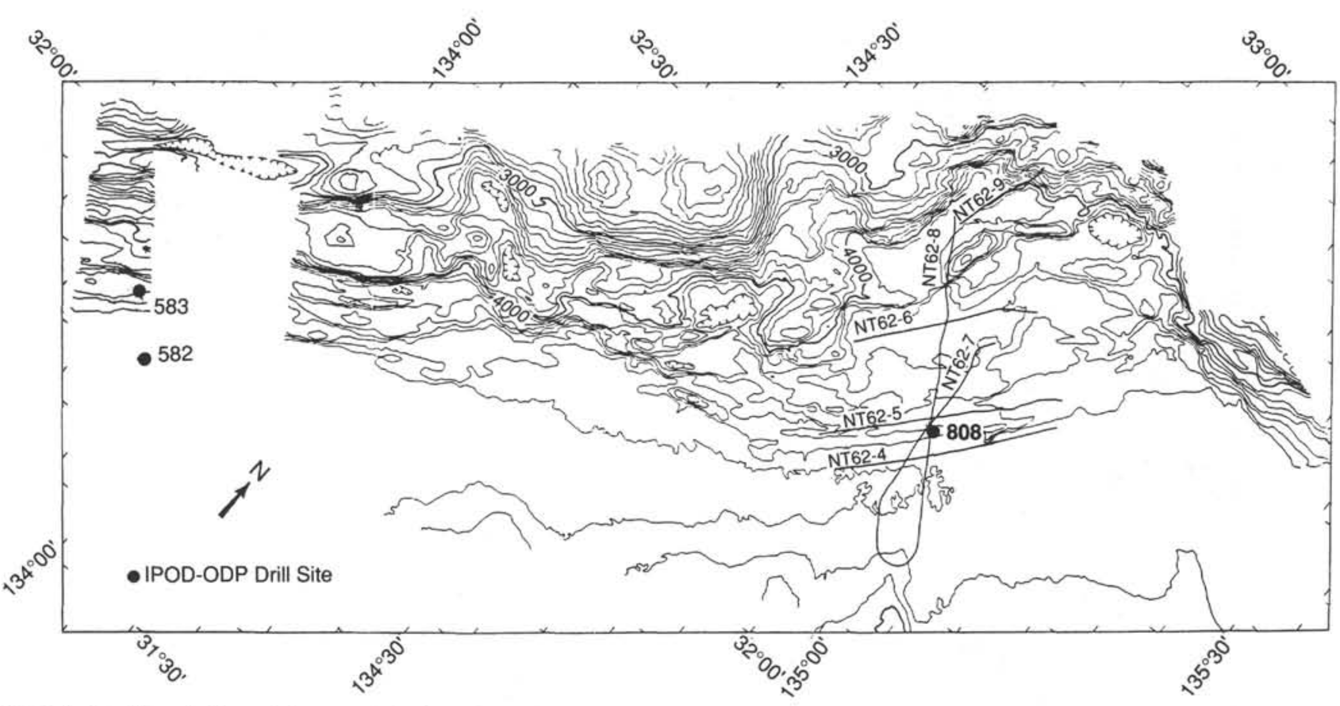

Figure 4. Sea Beam bathymetric map of the Leg 131 and Leg 87 sites. Contour interval is 100 m. Location of seismic profiles, NT62 series obtained by the *Fred Moore* is shown as solid line. The end of NT62-8 to the northwest, bounds the steep upper slope and gentle lower slope in this region (boundary approximated by 4000-m contour line).

are replaced by vaguely imaged landward-dipping reflectors. Folds associated with thrust faults are often clearly imaged, again within the frontal thrust packages.

Although there is much gross uniformity in structural styles of the western Nankai accretionary prism, there are noticeable local differences. Regional bathymetry of the Leg 131 site suggests that this area is composed of two slope gradients: an upper steep slope zone and a lower gentle slope zone (see Fig. 4). The origin of the upper steep zone is not clear, but some authors have attributed it to seamount indentation (Yamazaki and Okamura, 1989). Compared with the Leg 87 region, the gradient of the lower slope, namely the slope of the toe region, is much smaller: less than 2 degrees in the Leg 131 region and 4 to 6 degrees in the Leg 87 region, making the critical taper of the former to be about 3 to 4 degrees and that of the latter 8 to 10 degrees. In fact, the critical taper of about a 30-km-wide lower slope region of the Leg 131 area shows a distinctively smaller value than the rest of the western Nankai accretionary prism, indicating either a stronger accretionary wedge body and/or weaker friction along the décollement. Weaker friction at the décollement can be generally attributed to elevated pore pressure. Thus, we anticipated that there is a possibility that the Leg 131 area represents a zone of highest pore pressure and most active fluid migration among the different segments of the western Nankai accretionary prism.

The seismic line NT62-8 (Backpocket Fig. 2, Chapter 2, this volume) provides the basic structural framework of the drilling sites. Here the trench is about 14 km wide with a generally flat seafloor and a possible channel in the middle. At about 7 km from the outer margin of the trench fill, the trench floor becomes gradually elevated by about 10 m or so. At the same location, in the middle of the hemipelagic section, a reflector starts to emerge. Then, gradually toward the land, trench turbidite reflectors become tilted seaward and the first indication of faulting can be recognized at CMP 820. An anticline about 1.5 km in wavelength is imaged, the landward flank of which is bounded by an initial major thrust with 300-m displacement along the fault and 150-m vertical displacement. We can define this fault as the boundary between the proto-thrust zone and the imbricate thrust zone. The fault dips about 30 degrees and an upper hanging wall anticline is clearly defined. The top of the anticline is elevated about 120 m above the trench floor. Behind this anticline, a second major thrust can be defined as a reflector dipping at 20 degrees in the upper part and steepening with depth. Landward, the bottom-simulating reflector (BSR) starts to develop at a depth of 200 mbsf.

All the thrusts sole out to a reflector that develops at about 1000 mbsf and continues for about 30 km landward, where the reflector seems to step down to the boundary between the ocean crust and overlying sedimentary sequence. This continuous reflector, judging from the structural style and reverse polarity of the reflected wavelet, can be regarded as a main detachment zone (décollement). The décollement develops in the central part of the hemipelagic section, which is about 600 m thick. The hemipelagic section of this area differs in seismic character from the Leg 87 area. The section recognized in the profile NT62-8 shows two stratigraphic subdivisions: an upper reflective section and a lower transparent section, whereas the Leg 87 region is characterized by a three-fold stratigraphy; upper transparent sequence, middle reflective sequence, and lower transparent sequence.

The basement topography in the Leg 131 area is generally flat (Taira and Scientific Members, 1988) and the IZANAGI image (Fig. 2 in Chapter 2, this volume) clearly shows that lateral continuation of the toe thrust traces persist about 15 km along strike. We consider the two-dimensionality of the structure to be well documented in this region.

OBJECTIVES, MEASUREMENTS, AND INTEGRATION

The main objectives of scientific drilling during Leg 131 included elucidation of the following thematic issues:

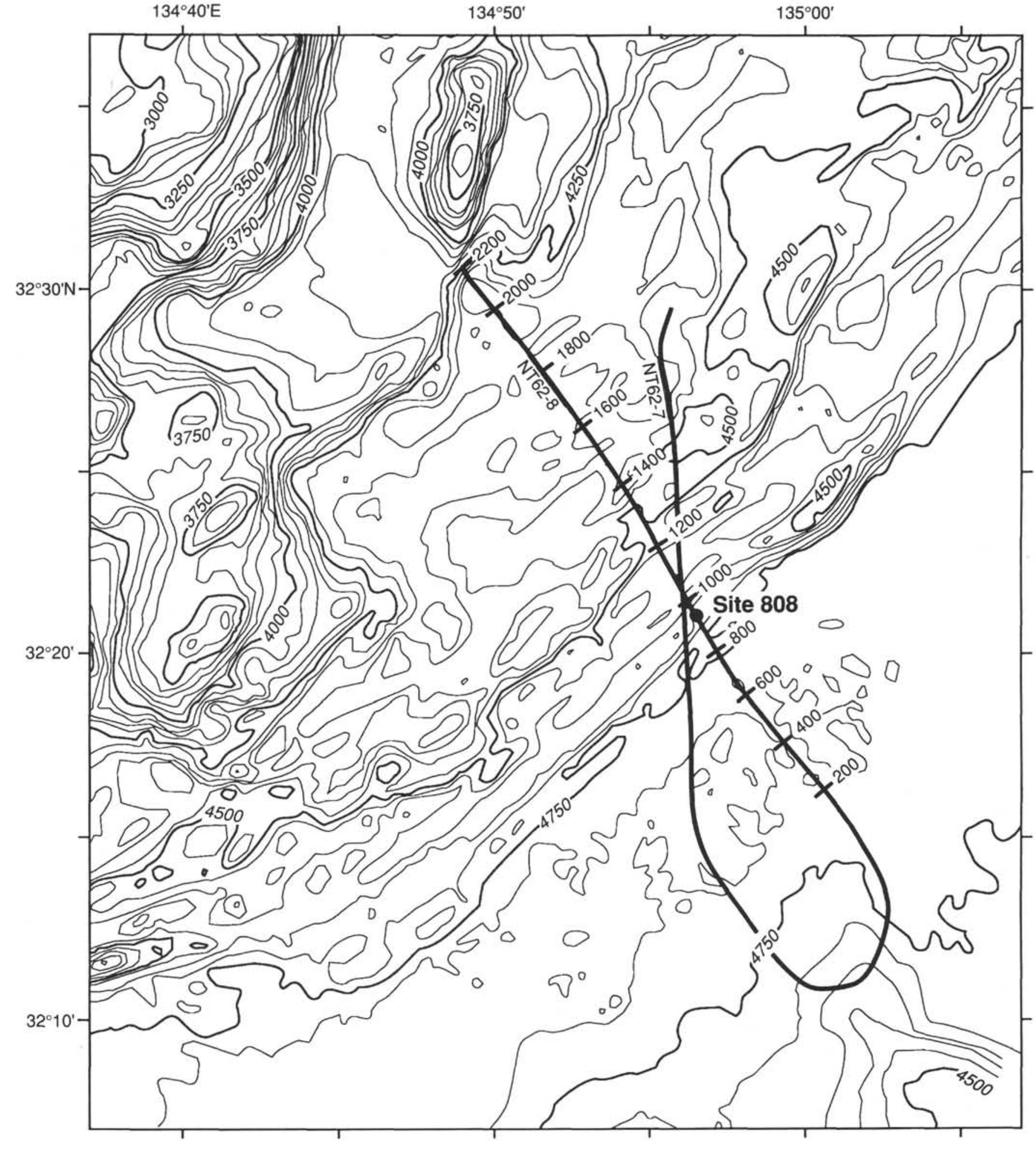

Figure 5. Sea Beam bathymetric map of the Leg 131 Site.

1. The influence of pore fluid and the hydrogeology of the accretionary prism;
2. The mechanical state and physical properties of deformed sediments;
3. The fabrics and structural styles of sediments before and after accretion.

These objectives are closely interrelated and were studied by a variety of methods on a range of spatial scales. Downhole experiments, wireline logging, and laboratory analyses of sedimentology, physical properties, and structural fabrics were closely coordinated. The sampling and measurement plan was made to cross-correlate these parameters as closely

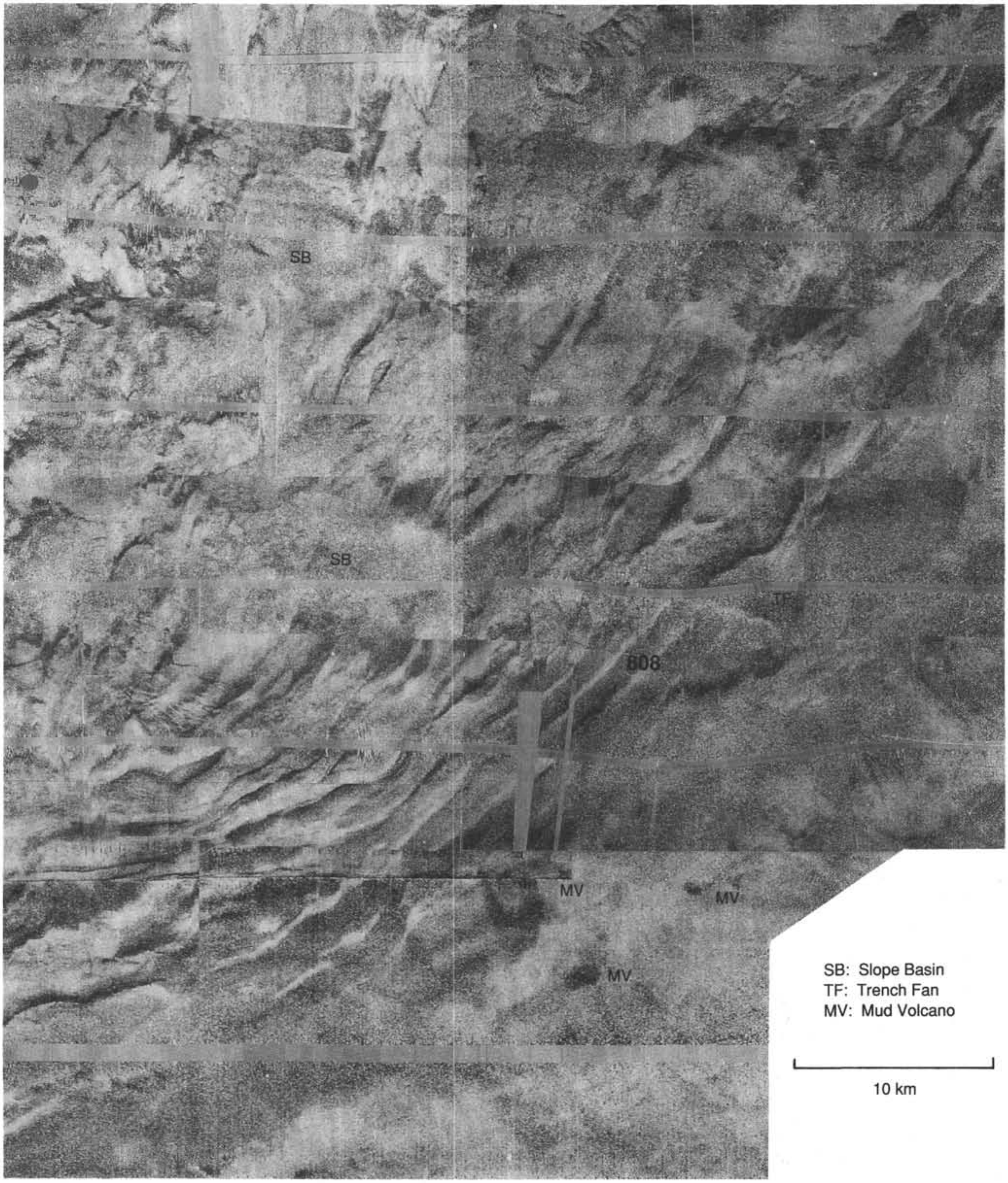

Figure 6. IZANAGI backscattering seafloor sonar image of the Leg 131 site. Note regularly spaced traces of thrust faults.

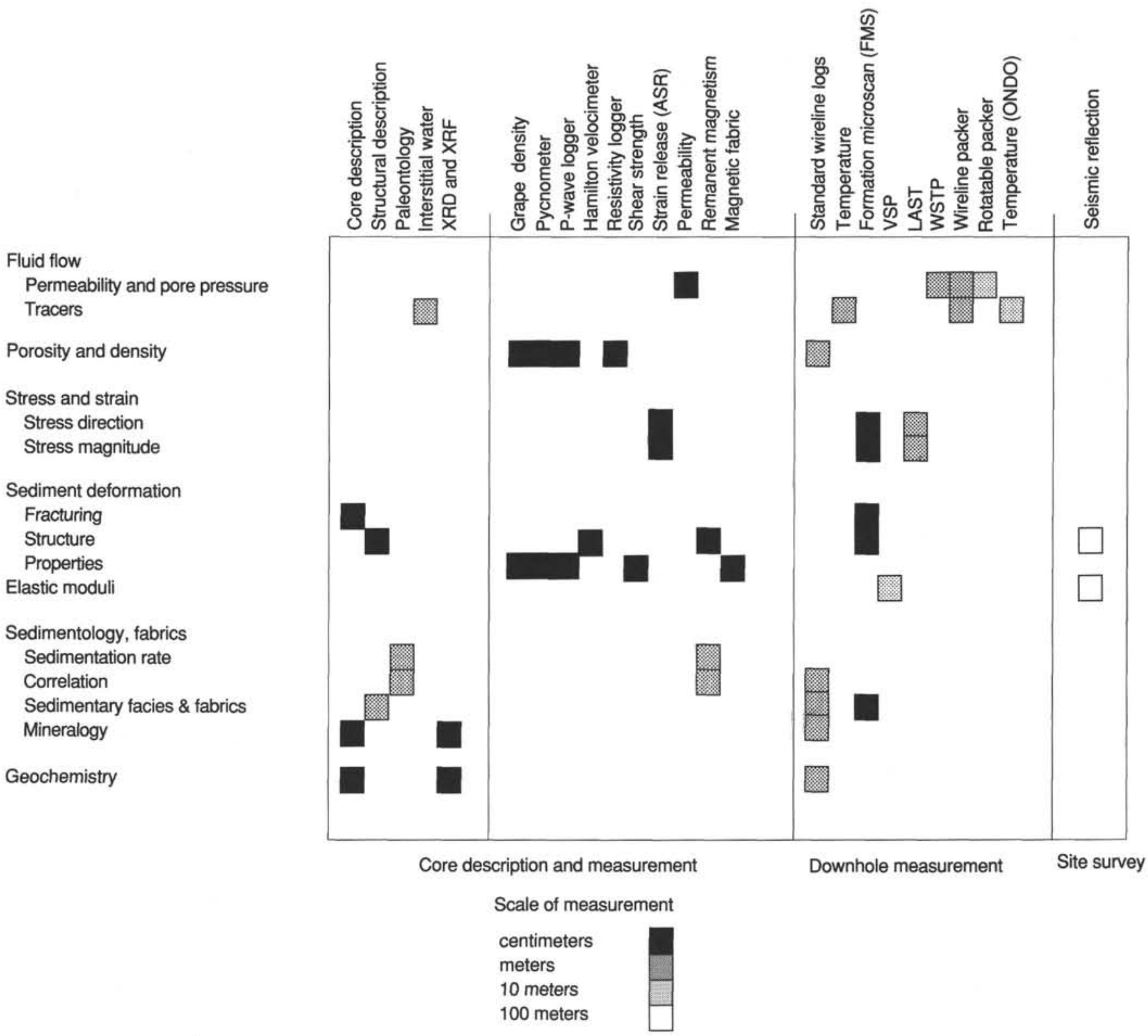

Figure 7. Interaction of the range of scientific objectives and the methodologies used to achieve them. The shading of the boxes expresses the range of different spatial scales that are investigated by different methods. XRD: X-ray diffraction. XRF: X-ray fluorescence.

as possible. Figure 7 indicates how these different measurements were combined to achieve a knowledge of eight primary aspects of accretionary prism development and evolution: (1) fluid flow; (2) porosity and density; (3) stress and strain; (4) elastic moduli; (5) sedimentology, structure and fabrics; (6) geochemistry; (7) stratigraphy; and (8) basement petrology and geochemistry.

Although detailed procedures for each measurement are included in the explanatory notes, it is useful to provide an overview of the significance of these parameters because this leg was designed to perform integrated and coordinated measurements, in a manner unprecedented in previous ocean drilling legs.

Fluid Flow and Thermal Structure

The extent and intensity of fluid flow strongly influence the evolution of structural styles, diagenetic alteration, and thermal structure of accretionary prisms (Westbrook and Smith, 1983; Brown and Westbrook, 1988). Direct measurement of these parameters is quite difficult. In Leg 131, we intended to determine whether fluid flow is localized along particular zones, and the time-variable nature of that flow (e.g., Sample and Moore, 1987; Henry et al., 1989). *In-situ* permeability and pore-pressure measurements with LAST (Lateral Stress and Temperature) tool, WSTP (Water Sampler, Temperature, Pressure) tool and drill-string packer were scheduled. The fluid geochemistry also contributed to the study of the source of the fluids and alteration processes within the prism.

The elucidation of thermal structure of the prism is an important contribution to the understanding of the fluid migration, physical property evolution, and diagenetic processes. The WSTP tool provided *in-situ* point values, and high-resolution downhole temperature logging recorded thermal structure of the borehole immediately after it was drilled.

A string of temperature and pressure sensors (ONDO experiment) was to be deployed at Site 808 to create a long-term observatory to augment the point sampling of this leg.

Porosity and Density

Porosity is directly related to the strength and the consolidation history of the sediments, as well as to other physical properties (Bray and Karig, 1985; Karig, 1986). Porosity and density were measured on a range of scales, and a comparison of laboratory measurements with borehole logs and seismic experiments was carried out.

Stress and Strain

These are vital parameters for understanding the structures observed in both cores and drill holes. Stress orientation was to be detected by borehole breakouts and fracture orientations with the formation microscanner (FMS). The state of stress in the borehole is directly related to strain indicators in the core. For these studies, attempts to orient cores were made with the multishot tool for APC cores, and paleomagnetic data for XCB and RCB cores. Careful observation was made on core-scale structural features following the guideline set by Lundberg and Moore (1986). Laboratory measurements using anisotropic strain-relaxation techniques were carried out for whole-round core samples. A special downhole tool, LAST, was developed to gain information on the state of stress in the shallower part of the prism.

Elastic Moduli

These parameters were estimated from both laboratory measurements and downhole measurements. Core measurements show the properties relative to individual structures of the core; the Sonic log and vertical seismic profile (VSP) show representative values for bulk volumes of the prism. These data were to be closely correlated and provided a comparative study with stress, strain, porosity, and density.

Sedimentology, Structure, and Fabrics

Sedimentological studies allow lithologic correlation and provide constraints on conditions prior to deformation. The nature of trench sedimentation and hemipelagic sedimentation was studied through sedimentary facies, mineralogy, and sedimentary geochemistry. Grain size and fabric study provided useful information for interpretations of mechanical and physical parameters.

Extensive studies on structures and fabrics of cores were conducted that detected important features such as faults, shear bands, veins, cleavages, and phacoids. These features were related to and interpreted with various other information.

Geochemistry

A detailed and extensive program of geochemical studies was scheduled for this leg including new instrumentation such as the Pressure Core Sampler (PCS). Interstitial fluid sampling was to be carried out both in laboratory and *in-situ* conditions. Geochemical studies were correlated closely to other parameters and provided key information on the nature of fluid flow and diagenetic processes.

Stratigraphy

Age assignment of the sedimentary sequence of Leg 131 was given by calcareous nannofossils. Paleomagnetic measurements complemented the biostratigraphy to provide well-constrained dating for the sedimentary sequence. Together with lithostratigraphic correlation these data aided interpretation of large-scale structural images obtained by seismic reflection profiling.

Basement Petrology and Geochemistry

Basement rocks obtained on this leg were the Shikoku Basin basaltic intrusives and extrusives. Petrological analysis and fluid samples obtained from the basement sequence provided valuable knowledge of alteration processes of back-arc basin crust and geochemical budget in the subduction zone.

GOALS OF LEG 131

The objectives of Leg 131 were to investigate the interplay of various parameters that influence the structural evolution of the accretionary prism, with special emphasis on hydrogeology. The drill site was selected to be the optimum place to study fluid flow and the state of pore pressure in the deeper part of the accretionary prism, especially at the fault and décollement zone.

The whole leg was designed to focus an integrated approach to the objectives. Therefore the sampling and measurements did not follow a "routine" approach. We intended that this leg provide very comprehensive, integrated, and meaningful results to the understanding of accretionary prism geology.

REFERENCES

Aalto, K. R., 1982. The Franciscan complex of northernmost California: sedimentation and tectonics. *In* Leggett, J. K. (Ed.), *Trench-Forearc Geology*. Geol. Soc. Spec. Publ. London, 10:495–520.

Aoki, Y., Kinoshita, H., and Kagami, H., 1986. Evidence of a low-velocity layer beneath the accretionary prism of the Nankai Trough; inference from a synthetic sonic log. *In* Kagami, H., Karig, D. E., Coulbourn, W., et al., *Init. Repts. DSDP,* 87: Washington (U.S. Govt. Printing Office), 727–735.

Aoki, Y., Tamano, T., and Kato, S., 1982. Detailed structure of the Nankai Trough from migrated seismic sections. *In* Watkins, J., and Drake, C. L. (Eds.), *Studies in Continental Margin Geology*. AAPG Mem., 34:309–322.

Ashi, J., Tokuyama, H., Yamamoto, F., Uyeki, T., Tukioka, H., and Taira, A., 1989. Detailed surface features of the Nankai accretionary prism obtained by IZANAGI oceanfloor imaging sonar system. *Prog. Abstr. Seismol. Soc. Jpn.,* 2:305.

Biju-Duval, B., Moore, J. C., et al., 1984. *Init. Repts. DSDP,* 78A: Washington (U.S. Govt. Printing Office).

Bray, C. J., and Karig, D. E., 1985. Porosity of sediments in accretionary prisms, and some implications for dewatering processes. *J. Geophys. Res.,* 90:768–778.

Brown, K., and Westbrook, G. K., 1988. Mud diapirism and subcretion in the Barbados Ridge accretionary complex: the role of fluids in accretionary processes. *Tectonics,* 7:613–640.

Byrne, T., 1984. Early deformation in melange terranes of the Ghost Rocks Formation, Kodiak Islands, Alaska. *In* Raymond, L. A. (Ed.), *Melanges: Their Nature, Origin, and Significance:* Geol. Soc. Am. Spec. Pap., 198:21–52.

Chamot-Rooke, N., Renard, V., and Le Pichon, X., 1987. Magnetic anomalies in the Shikoku Basin: a new interpretation. *Earth Planet. Sci. Lett.,* 83:214–228.

Curtis, D. M., Echols, J., et al., 1980. Lithofacies at the Shikoku and Parece Vela Basins. *In* Klein, G. deV., and Kobayashi, K., et al., *Init. Repts. DSDP,* 58: Washington (U.S. Govt. Printing Office), 701–710.

Davis, D. M., Suppe, J., and Dahlen, F. A., 1983. Mechanics of fold-and-thrust belts and accretionary wedges. *J. Geophys. Res.,* 88:1153–1172.

Fisher, D., and Byrne, T., 1988. Structural evolution of underthrusted sediments, Kodiak Islands, Alaska. *Tectonics,* 6:755–793.

Henry, P., Lallemant, S. J., Le Pichon, X., and Lallemand, S. E., 1989. Fluid venting along Japanese trenches, tectonic context and thermal modeling. *Tectonophysics,* 160:277–292.

Kaiko I Research Group, 1986. Taira, A., and Tokuyama, H. (Eds.), *Topography and Structure of Trenches Around Japan-Data Atlas of Franco-Japanese Kaiko Project, Phase I:* Tokyo (Univ. of Tokyo Press).

Karig, D. E., Ingle, J. C., Jr., et al., 1975. *Init. Repts DSDP,* 31: Washington (U.S. Govt. Printing Office).

Karig, D. E., 1986. Physical properties and mechanical state of accreted sediments in the Nankai Trough, Southwest Japan Arc. *In* Moore, J. C. (Ed.), *Structural Fabrics in Deep Sea Drilling Project Cores from Forearcs.* Mem. Geol. Soc. Am., 66:117–133.

Karig, D. E., and Angevine, C. L., 1986. Geologic constraints on subduction rates in the Nankai Trough. *In* Kagami, H., Karig, D. E., and Coulbourn, W. E., et al., *Init. Rept. DSDP,* 87: Washington (U.S. Govt. Printing Office), 789–796.

Karig, D. E., and Lundberg, N., 1990. Deformation bands from the toe of the Nankai accretionary prism. *J. Geophys. Res.,* 95:9099–9109.

Kinoshita, H., and Yamano, M., 1986. The heat flow anomaly in the Nankai Trough area. *In* Kagami, H., Karig, D. E., Coulbourn, W. C., et al., *Init. Repts DSDP,* 87: Washington (U.S. Govt. Printing Office, 737–743.

Kobayashi, K., and Nakada, M., 1978. Magnetic anomalies and tectonic evolution of the Shikoku inter-arc basin. *J. Phys. Earth,* 26:391–402.

Leggett, J. K., McKerrow, W. S., and Casey, D. M., 1982. The anatomy of a Lower Paleozoic accretionary forearc: the Southern Uplands of Scotland. *In* Leggett, J. K. (Ed.), *Trench-Forearc Geology.* Geol. Soc. Spec. Publ. London, 10:496–520.

Le Pichon, X., Iiyama, T., Chamley, H., Charvet, J., Faure, M., Fujimoto, H., Furuta, T., Ida., Y., Kagami, H., Lallemant, S., Leggett, J., Murata, A., Okada, H., Rangin, C., Renard, V., Taira, A., and Tokuyama, H., 1987a. Nankai Trough and fossil Shikoku Ridge results of Box 6 Kaiko Survey. *Earth Planet. Sci. Lett.,* 83:186–198.

Le Pichon, X., Iiyama, T., Boulègue, J., Charvet, J., Faure, M., Kano, K., Lallemant, S., Okada, H., Rangin, C., Taira, A., Urabe, T., and Uyeda, S., 1987b. Nankai trough and Zenisu Ridge: a deep-sea submersible survey. *Earth Planet. Sci. Lett.,* 83:285–299.

Lundberg, N., and Moore, J. C., 1986. Macroscopic structural features in Deep Sea Drilling Project cores from forearc regions. *In* Moore, J. C. (Ed.), *Structural Fabrics Preserved in Deep Sea Drilling Project Cores From Forearcs:* Mem. Geol. Soc. Am., 166:13–44.

Marlow, M., Lee, H., and Wright, A., 1984. Physical properties of sediment from the Lesser Antilles margin along the Barbados Ridge: results from Deep Sea Drilling Project Leg 78A. *In* Biju-Duval, B., Moore, J. C., et al., *Init. Repts. DSDP,* 78A: Washington (U.S. Govt. Printing Office), 549–558.

Mascle, A., Moore, J. C., et al., 1988. *Proc. ODP, Init. Repts.,* 110: College Station, TX (Ocean Drilling Program).

Moore, G. F., Shipley, T. H., Stoffa, P. L., Karig, D. E., Taira, A., Kuramoto, S., Tokuyama, H., and Suyehiro, K., 1990. Structure of the Nankai Trough accretionary zone from multichannel seismic reflection data. *J. Geophys. Res.,* 95:8753–8765.

Moore, J. C., 1989. Tectonics and hydrogeology of accretionary prisms: role of the decollement zone. *J. Struct. Geol.,* 11:95–106.

Moore, J. C., and Lundberg, N., 1986. Tectonic overview of Deep Sea Drilling Project transect of forearcs. *In* Moore, J. C. (Ed.), *Structural Fabrics in Deep Sea Drilling Project Cores from Forearcs.* Mem. Geol. Soc. Am., 166:1–12.

Moore, J. C., Mascle, A., Taylor, E., Andreieff, P., Alvarez, F., Barnes, R., Beck, C., Behrmann, J., Blanc, G., Brown, K., Clark, M., Dolan, J., Fisher, A., Gieskes, J., Hounslow, M., McLellan, P., Moran, K., Ogawa, Y., Sakai, T., Schoonmaker, J., Vrolijk, P., Wilkens, R., and Williams, C., 1988. Tectonics and hydrogeology of the northern Barbados Ridge: results from Ocean Drilling Program Leg 110. *Geol. Soc. Am. Bull.,* 100:1578–1593.

Nasu, N., et al., 1982. Multi-channel Seismic Reflection Data across Nankai Trough. *IPOD-Japan Basic Data Series,* 4. Ocean Res. Inst., Univ. of Tokyo.

Sample, J. C., and Moore, J. C., 1987. Structural style and kinematics of an underplated slate belt, Kodiak and adjacent islands, Alaska. *Geol. Soc. Am. Bull.,* 99:7–20.

Seno, T., 1977. The instantaneous rotation of the Philippine Sea plate relative to the Eurasian plate. *Tectonophysics,* 42:209–226.

Shi, Y., and Wang, C.-Y., 1988. Generation of high pore pressures in accretionary prisms: inferences from the Barbados Subduction Complex. *J. Geophys. Res.,* 93:8893–8909.

Shih, T. C., 1980. Magnetic lineations in the Shikoku Basin. *In* Klein, G. deVries, and Kobayashi, K., et al., *Init. Rept. DSDP,* 58: Washington (U.S. Govt. Printing Office), 783–788.

Shiono, K., 1988. Seismicity of the SW Japan arc - subduction of the young Shikoku Basin. *Mod. Geol.,* 12:449–464.

Shipboard Scientific Party, 1986. Site 582. *In* Kagami, H., Karig, D. E., Coulbourn, W. C., et al., *Init. Repts. DSDP,* 87: Washington (U.S. Govt. Printing Office), 35–122.

Taira, A., Katto, J., Tashiro, M., Okamura, M., and Kodama, K., 1988. The Shimanto Belt in Shikoku, Japan -Evolution of Cretaceous to Miocene accretionary prism. *Mod. Geol.,* 12:5–46.

Taira, A., and Niitsuma, N., 1986. Turbidite sedimentation in the Nankai Trough as interpreted from magnetic fabric, grain size, and detrital modal analyses. *In* Kagami, H., Karig, D. E., Coulbourn, W. C., et al., *Init. Repts. DSDP,* 87: Washington (U.S. Govt. Printing Office), 611–632.

Taira, A., and the Scientific Members of the Expedition, 1988. *Preliminary Report of the Hakuho-Maru Cruise KH86-5.* Ocean Res. Inst., Univ. of Tokyo.

Taira, A., and Tashiro, M., 1987. Late Paleozoic and Mesozoic accretion tectonics of Japan and eastern Asia. *In* Taira, A., and Tashiro, M. (Eds.), *Historical Paleogeography and Plate Tectonic Evolution of Japan and Eastern Asia:* Tokyo (Terra Publ.), 1–47.

Taira, A., Tokuyama, H., and Soh, W., 1989. Accretion tectonics and evolution of Japan. *In* Ben-Avraham, Z. (Ed.), *The Evolution of the Pacific Ocean Margins:* Oxford (Oxford Univ. Press), 100–123.

Watkins, J. S., Moore, J. C., et al., 1982. *Init. Repts. DSDP,* 66: Washington (U.S. Govt. Printing Office).

Westbrook, G. K., and Smith, M. J., 1983. Long décollements and mud volcanoes: evidence from the Barbados Ridge Complex for the role of high pore-fluid pressure in the development of an accretionary complex. *Geology,* 11:279–283.

Yamano, M., Uyeda, S., Aoki, Y., and Shipley, T. H., 1982. Estimates of heat flow derived from gas hydrates. *Geology,* 10:339–343.

Yamazaki, T., and Okamura, Y., 1989. Subducting seamounts and deformation of overriding forearc wedges around Japan. *Tectonophysics,* 160:207–229.

Ms 131A-101